

# Comparison of Simple Models for RPC Weighting Fields and Potentials

Stefan Rossegger, Bernhard Schnizer, Gunther Schweitzer

*Institut für Theoretische Physik, Technische Universität Graz, Petersgasse 16,  
A-8010 Graz, Austria, Phone (+43 316 873-81 73), Fax -8678*

---

## Abstract

A theoretical tool is provided for investigating the weighting fields and potentials in simple models approximating the electrode configurations in Resistive Plate Chambers (RPC's). The influence of dielectrics on the signals is neglected. Formulae are derived by conformal maps and implemented in user-friendly *Mathematica* programs available on Schnizer's website. The models are a plane condenser with a gap in the upper electrode (left side on tension), a plane condenser with a semi-infinite upper electrode on tension (corresponding to an infinite gap) and a plane condenser with a strip under tension on the upper electrode (corresponding to gaps of zero width). For the last model closed analytic expressions can be given for mapping functions, fields and potentials. The other two require a numerical or approximate analytical function inversion. There is also a program for comparing the results of these various models.

*Key words:* RPC, Field computations, Conformal maps, Weighting fields  
*PACS:* 41.20.Cv, 02.70.Wz

---

## 1 Introduction

Signals in particle counters are induced in the electrodes by the motion of the electronic (or ionic) charge cloud generated by the ionizing action of the primary particle, multiplied and set in motion by a static high voltage tension. These signal currents are conveniently treated by Ramo's theorem [1]. This

---

*Email address:* [schnizer@itp.tu-graz.ac.at](mailto:schnizer@itp.tu-graz.ac.at) (Stefan Rossegger, Bernhard Schnizer, Gunther Schweitzer).

*URL:* [http://www.itp.tu-graz.ac.at/~schnizer/Theory\\_of\\_Chambers/](http://www.itp.tu-graz.ac.at/~schnizer/Theory_of_Chambers/)  
(Stefan Rossegger, Bernhard Schnizer, Gunther Schweitzer).

theorem relates the current flowing from (or to) the grounded electrode to the static (weighting) field excited by that electrode under tension in the absence of the charge. It has been extended to configurations containing weakly conducting dielectrics as for example Resistive Plate Chambers or Gas Microstrips by Riegler [2] using the quasi-static approximation, [3]-[5]. These analyses show that contributions due to a weak conductivity of the media to the signals are of the order of  $D\sigma/v\epsilon$  ( $\sigma$ , conductivity,  $\epsilon$  dielectric constant of the medium,  $v$  velocity of the inducting electron (or ion) avalanche,  $D$  detector width); in many cases this dimensionless parameter is small as compared to unity. The influence of the capacitance of a dielectric layer (relative dielectric constant  $=\epsilon_r$ ) crossed by a signal is of the order of  $(\epsilon_r - 1)/(\epsilon_r + 1)$ ; this is not so small, in general, but a more detailed analysis shows that additional factors limit the magnitude of this contribution to 10% at most [6].

So it is mainly the configuration of the electrodes disregarding the media, which determines the weighting field, in turn giving the current flowing from the electrodes after the velocity  $v$  has been given. Since the anode strips are long as compared to the width of the gas gap, the configurations can be regarded as two-dimensional. Here the fields of three simple configurations are treated by conformal maps.

The formulae derived by this method are implemented in publicly available *Mathematica* programs to calculate and plot the fields and the induced currents. The three simple models are: a plane condenser with a gap in the upper electrode (left side under tension), a plane condenser with a semi-infinite upper electrode under tension and a plane condenser with a strip under tension on the upper electrode. The other electrodes are grounded. The position of the strip and the edge of the semi-infinite electrode may be shifted in order to allow a direct comparison with the "Split Condenser" model, where the upper electrode is split into two by a gap. Two of the above models have been presented before [7]; but the theory has been reworked and extended; new programs have been prepared and tested over ranges of the geometric parameters. Long write-up notebooks explain in detail the working of the conformal maps and the derivation of approximations.

The "Voltage Strip" model has the advantage that all quantities are expressed by closed simple analytic expressions. So they are particularly useful in problems where many cases must be studied as, for example, in optimization studies. The omission of the gaps present in the real device may lead to deviations between the theoretical and the real field values in the neighbourhood of the gaps. The programs described here permit one to assess these errors.

The programs may be downloaded from the website given on the first page.

## 2 Conformal Maps, complex fields and potentials

The real configurations (of the simple models) in the  $z$ -plane ( $z = x + iy$ ) are mapped to an infinite strip in the  $W$ -plane ( $W = U + iV$ ) by the chain of conformal maps

$$z = f(W) = f_3(f_2(f_1(W))), \quad W = f^{-1}(z) = f_1^{-1}(f_2^{-1}(f_3^{-1}(z))), \quad (1)$$

which are described in the following sections. The electric field in this strip is uniform.

The electric fields may be derived from real potentials in the usual way. These potentials as well as the fields may be extended to complex ones by the Cauchy-Riemann equations [8].

$$\Psi(W) = \Psi_1 + i\Psi_2 = -iV_0W/\pi \quad (2)$$

$$\Phi(z) = \Phi_1 + i\Phi_2 := \Psi(W) \quad (3)$$

$$E(W) = E_U + iE_V = -(d\Psi/dW)^* = -iV_0/\pi \quad (4)$$

$$E_z = E_x + iE_y = -(d\Phi/dz)^* \quad (5)$$

$$= -iV_0/[\pi(dz/dW)^*] = -(d\Psi/dW)^* \cdot (dW/dz)^*. \quad (6)$$

$E(W)$  is the uniform complex electric field in the simple infinite plane condenser.  $E_z$  is the complex electric field in the configuration under consideration in the  $z$ -plane. In view of the conformal map  $W = f(z)$  it may be represented as a function of either  $z$  or  $W$ . The formulae above were already given in [7]; but in this reference the formulae representing the complex field as a derivative of the complex potential contain an erroneous factor  $i$ .

In all cases the infinite plane condenser is mapped to the upper half of the complex  $t$ -plane by the transformation

$$t = r + is = f_1(W) = e^W, \quad (7)$$

such that the electrode  $V = 0$  ( $\pi$ ) becomes the half-ray  $s = 0$ ,  $r > (<) 0$ . The real configuration (in the  $z$ -plane) is mapped to the  $t'$ -plane by  $t' = f_3^{-1}(z)$  such that the electrodes become the  $s'$ -axis. The  $t$ -plane is mapped to the  $t'$ -plane by  $t' = f_2(t)$ .  $f_2$  and  $f_3$  are typical for each configuration and are given below in the subsections.

## 2.1 Plane condensor with shifted voltage strip

A voltage  $V_0$  is impressed along a strip of width  $w$  attached to the upper electrode  $y = D$ . The strip extends from  $x = c - w$  to  $x = c$ ; the remaining parts of this electrode and the lower one are grounded. The shift  $c$  has been introduced so that the right edge of the strip may be matched with that of another configuration for the sake of comparison. Closed expressions can be given for all the mappings and their inverses, for the potentials and the fields. The mapping functions are:

$$t' = r' + is' = f_2(t) = -(t\alpha^2 - 1)/(t - \alpha^2); \quad \alpha = e^{\pi w/4D}, \quad (8)$$

$$z = f_3(t') = D/\pi \ln(t') + c. \quad (9)$$

$f_2(t)$  maps the  $t$ -plane to the  $t'$ -plane so that the potential  $\Phi = V_0$  extends from  $s' = -1/\alpha^2$  to  $s' = -\alpha^2$ .  $f_3(t')$  is similar to  $f_1^{-1}$ ; it maps the half-plane  $s \geq 0$  to the upper half of the  $z$ -plane. The total map and its inverse may be given as closed analytic expressions:

$$z = f(W) = \frac{D}{\pi} \ln \left[ \frac{\sinh(\pi w/4D + W/2)}{\sinh(\pi w/4D - W/2)} \right] + c - \frac{w}{2} \quad (10)$$

$$W = f^{-1}(z) = \ln \left[ \frac{\cosh[\pi(z - c + w)/2D]}{\cosh[\pi(z - c)/2D]} \right]. \quad (11)$$

The complex potential is  $\Phi(z) = -iV_0W/\pi$ , where the preceding formula is inserted for  $W$ . The complex electric field is:

$$E_z(z) = i \frac{V_0}{2D} \left[ \tanh[\pi(z^* - c)/2D] - \tanh[\pi(z^* - c + w)/2D] \right] \quad (12)$$

$$E_z(W) = i \frac{V_0}{2D} \frac{2 \cosh(W^*) - (\alpha^2 + 1/\alpha^2)}{\alpha^2 - 1/\alpha^2}. \quad (13)$$

The above formulae are used in the *Mathematica* notebook *CondShVoSt.nb* to compute and draw field distributions. The mappings are discussed in more detail in the long write-up notebook *CondVoStLW.nb*.

Putting  $c = w/2$  gives the formulae for the strip centred at  $z = iD$  presented in [7]. There is a special notebook for this case called *CondVoSt.nb*. Unfortunately, there are some errors in [7]. The arguments in the expression for the complex potential should read  $\bar{z}_\pm/2$  in place of  $\pi\bar{z}_\pm/2D$ . The expression for the real part of  $\Phi(z)$  is correct. But its range of validity is more restricted than that given above, since the principal branch of the *arctan* is more limited

than that of the logarithm. This problem does not at all apply to the real or complex field representations.

## 2.2 Plane condensor with shifted semi-infinite upper electrode

The lower electrode,  $y = 0$ , extends to infinity in both directions and is grounded. The upper electrode,  $y = D$ , is at potential  $V_0$ ; it is a semi-infinite plane extending to infinity at the left; its edge is at  $x = b$ . This parameter has been introduced so that this edge may be matched with that of another configuration.

$$z = f_3(t') = D/\pi (1 + \ln t' + t') + b \quad (14)$$

$$= (D/\pi) (1 + W + e^W). \quad (15)$$

The function in the first line above maps all the electrodes to the  $r'$ -axis. The second line maps the real configuration to the infinite plane condensor in the  $W$ -plane. No single-valued analytic expression can be given for its inverse. *Mathematica* turns out an inverse using a function `ProductLog[]`. However this function is not single-valued and leads to troubles. So we found it more expedient to find the total inverse function  $W = f^{-1}(z)$  by Newton's method. This works without problems with the following starting values :  $1.2 \operatorname{sign}(\operatorname{Re}(z) - D) + i\pi/2$ .

No closed expression can be given for  $\Phi(z)$  or  $E_z$ . Each value of these quantities is calculated from eqs.(2) to (5) after the value  $W$  belonging to a given  $z$  has been found according to (1). In particular, the electric field is computed by the following formula resulting from (6):

$$E(W) = -i(V_0/D) 1/(1 + e^{W*}). \quad (16)$$

The expressions given above are used in the Mathematica notebook *CondSh-SemInf.nb* to compute and draw potential and field distributions.

## 2.3 Plane condensor with a gap in the upper electrode

This model was introduced previously, [7], but, in the mean-time, it was found necessary to correct and amend the presentation. The configuration consists of two parallel infinite, ideally conducting planes having a distance  $D$ ; the lower one,  $y = 0$ , is continuous; the upper one,  $y = D$ , consists of two semi-infinite planes separated by a gap extending from  $x = -g/2$  to  $x = g/2$ . The left one is at potential  $\Phi = V_0$ . The other one and that at  $y = 0$  are grounded. The

mapping function is given in [10]. The geometry, more precisely, the ratio  $g/D$  determines a parameter  $p$ , which is the root of the following equation:

$$\frac{p^2 - 1}{2p} + \ln p = \frac{\pi g}{2D} ; \quad (17)$$

which in turn gives a parameter  $\alpha$

$$\alpha := (p - 1)^2/p, \quad (18)$$

occurring in the mapping function

$$z = f_3(t') = \frac{D}{\pi} \left[ \ln t' + \alpha \left( \frac{1}{2} - \frac{1}{1+t'} \right) \right]. \quad (19)$$

This maps the upper half of the  $t'$ -plane to the real condenser.  $p$ , the root of eq.(17) is found numerically. Graphs and approximate functions for  $p$  and  $\alpha$  as functions of  $g/D$  are given in the appendix.

The inverse function  $t' = f_3^{-1}(z)$  is found numerically by Newtons method in most cases. In order to ensure convergence, starting values  $t'_0$  are selected in dependence on  $z$ : For  $y \geq D \wedge x \geq 0$ :  $t'_0 = -(p+1)/2 + 0.2i$ ;  $x < 0$ :  $t'_0 = -(1/p+1)/2 + 0.2i$ ; for  $0 \leq y < D \wedge x \leq 0$ :  $t'_0 = 0.2i$ ;  $x > 0$ :  $t'_0 = 1.2i$ . The electrode unter tension is mapped to  $0 \leq s' \leq 1$ . This interval is mapped in turn to the half-ray  $s < 0$  by:  $t' = f_2(t) = t/(1-t)$ .  $t = f_1(W) = e^W$ ,  $f_2(t)$  and  $f_3(t')$  are used in eq.(1).

For positions  $z$  within the condenser far at the left, the numeric inversion leading to  $t' = f_3^{-1}(z)$  runs into trouble. In the appendix an approximate analytic expression is found for that part of the  $z$ -plane:

$$\begin{aligned} t' &= f_{3a}^{-1}(z) = & (20) \\ &= \frac{\beta (2 + 8\alpha\beta - 2\alpha\beta^2 + 11\alpha^2\beta^2 - 2\alpha^2\beta^3 + 3\alpha^3\beta^3)}{2 (1 + 5\alpha\beta - 2\alpha\beta^2 + 9\alpha^2\beta^2 - 4\alpha^2\beta^3 + 6\alpha^3\beta^3 - 2\alpha^3\beta^4 + \alpha^4\beta^4)} \\ \beta &:= e^{\pi z/2D + \alpha/2}, \quad \Re(z) < -1.05g, \quad 0 \leq \Im(z) \leq D. \end{aligned}$$

No closed expressions can be given for  $\Phi(z)$  or  $E(z)$ . Every evaluation of these quantities is done by calculating the value  $W$  belonging to a given value  $z$ . Then the potential is computed from eqs.(2) and (3); the electric field from (4) and (6):

$$E(z) = \frac{iV_0}{D} \left[ \frac{p (e^W - 1)}{p + (p-1)^2 (e^W - e^{2W})} \right]^* . \quad (21)$$

The above formulae are used in the *Mathematica* notebook *SplitCond.nb* to compute and draw field distributions and induced currents. More details on the derivations and maps can be found in the *Mathematica* notebook *SplitCondLW.nb*.

### 3 The Mathematica programs

The theory has been implemented in user-friendly *Mathematica* notebooks, whose names have been given above, which are displayed at [http://www.itp.tu-graz.ac.at/~schnizer/Theory\\_of\\_Chambers/Plane\\_Geometries](http://www.itp.tu-graz.ac.at/~schnizer/Theory_of_Chambers/Plane_Geometries). Default values are inserted for the values of all variables, so that these notebooks may be run as downloaded to compute and draw the potential and field distributions, and other interesting quantities listed below. An example of a figure prepared by each of the program notebooks is shown in Fig.1. There are many more figures provided in the notebooks! Indeed, the following tasks are performed in each notebook.

- (1) Drawing the equipotential and field lines of the interesting parts of the configuration. Drawing the normal electric field component along the (lower and upper) electrodes.
- (2) Drawing the equipotential and field line through a point selected by the user. The values of the potential and of the electric field components at that points are printed.
- (3) The currents induced on the main electrode for a list of vertical trajectories of the point charge representing the electronic or ionic cloud in uniform motion.
- (4) The current induced on the main electrode for a vertical trajectory of the point charge selected by the user.
- (5) A perspective drawing of the absolute value,  $|\vec{E}|$ , and of the vertical electric field component  $E_y$  of the interesting parts of the configuration.

The user may change the voltage and the geometric parameters of the electrode configuration to his own needs in each notebook. The corresponding cells of the notebook are shaded in cyan. The variables and commands are commented extensively to guide the unacquainted user. The variables in different programs have got different names inasmuch as the first two letters of each name are typical for the notebook: vs for the Voltage Strip model, cv for the Shifted Voltage Strip model, sc for the Split Condensator, hu for the Semiinfinite model. So several programs may be run in the same kernel without interference and the pictures or values may be juxtaposed or superimposed for comparison. But the programs of these four different notebooks have very similar structure; so it is easy to switch mentally from one notebook to the other; also the names of corresponding variables or commands performing the same tasks have names

with the same ending. Some results of these notebooks are shown in the next section.

A long write-up notebook, whose name ends with LW, is provided for two of the program notebooks, in which the derivations and the maps are explained extensively. But in these notebooks the naming of variables has not been done in the discriminating fashion adopted for the other program notebooks so that it is recommended to use these completely alone in a kernel.

The three notebooks, each one belonging to one of the three configurations, have been named at the end of the corresponding subsection of sect. 2.

A notebook comparing the results of all three notebooks got the name *Comparisons.nb*. This notebook contains the essential parts of the three notebooks just mentioned. Though the contents of these sections are hidden, the instructions contained therein are executed. At the beginning of the notebook *Comparisons.nb* there is a head containing parameters of the configurations to be compared. All these variables and commands start with the letters com. The input cells (marked in red, the user may change the numbers at will) control the input cells of the notebook sections corresponding to the three models; this ensures that the geometries of these match; in particular, the position of the edge common to all is the same as can be seen from the figures.

A notebook called *Animation.nb* shows the evolution of the potential and field distribution as the gap widths grows and shrinks; the same figures are also contained in *Animation.gif*.

## 4 Comparisons and discussion

Most figures rendered by the programs are in colors; so they are easier to view and comprehend than those given here in black, gray and white.

In the left column of Fig.1 the potential and field distributions in the three models are displayed for a given configuration, whose parameters are given in the caption. The model with the gap is the most realistic of the three; the other two represent the two limiting cases with zero gap width, infinite gap width respectively. The lower two figures of the right column display the superposition of the field distributions of two configurations. Some inaccuracies which may occur are explained in the caption.

In Fig.2 the field and potential line passing through a given point (which may be selected by the user) are plotted. The program prints the values of the potential and the electric field components at this point; these numbers



are given in the caption. These values agree quite well for points whose  $x$ -coordinate is around that of the centre of the strip. The field values computed from the Voltage Strip model differ appreciably from those resulting from the other two models if this  $x$ -coordinate is near that of the edge or outside the strip. This is understandable since the Voltage Strip model has a conducting plane above the charge, whereas the other models are open to free space.

In Fig.3 and 4 the values of the normal field components at the electrodes are plotted. These become infinite at the edges. So the values at and near these points are certainly too large. If one has got a realistic estimate of the radius of curvature of the edges one may drop those parts of the curves exceeding field values above those corresponding to a cylinder with that radius.

In Figs.5 and 6 the current induced in the gray electrode by a moving charge is shown. In Fig.5 this is done for a single trajectory having the same distance from the right hand edge of the electrode; the results of all three models are superimposed in the lower plot of this figure. In Fig.6 several trajectories and the corresponding currents are shown. Corresponding trajectories have been selected so that they have the same distance from the gray edge in each model. The corresponding currents are displayed below each model. It is impossible to collect all currents into one plot here. But in the notebook *Comparisons.nb* this can be done by distinguish the trajectories by color and the models by the type of dashing. From the pertinent plot in this notebook we draw some rough conclusions in comparing the current induced on the left electrode of the Split Condensor to that obtained from the corresponding trajectory in the other models. If the charge moves under the left electrode, the other models give good agreement. If the trajectory hits the edge, then the Voltage Strip model underestimates the current, while the Semiinfinite model gives good agreement. If the charge is at the centre of the gap separating the electrodes, then the Semiinfinite model overestimates the current a little, while the Voltage Strip model severely underestimates the current. If the trajectory is pointed to the edge of the right hand electrode, then the Semiinfinite model overestimates the current, the Voltage Strip model underestimates it. The deviations are about the same, except for the case where the charge is in the immediate neighbourhood of the edge. But one expects that there the Split Condensor model gives a value, which is too high, since in reality the curvature of the strip edge will not be infinite. If the charge moves under the grounded electrode, the current induced in the gray electrode is in good agreement with the Voltage Strip model, while the Semiinfinite model gives a large overestimate. All this results may also be gleaned from Fig.6. They are in agreement with physical expectations.

Of course, the relative magnitude of the two parameters  $D$  and  $g$  will influence the domains of validity of the other two models appreciably. It is just the aim of the programs prepared by the authors and published on the website to

enable users to perform their own checks for their own configurations.

It is planned to develop the programs in several directions. In particular, we are trying to implement a routine giving a perspective plot of the deviations. So users are encouraged to check our website periodically. They may request to be put on our mailing list, so that they will be informed of changes in the programs.

## 5 Acknowledgements

The authors thank Prof. M. Regler, HEPHY, Vienna, for suggesting this line of research and W. Riegler, CERN, Geneva, Switzerland for helpful discussions.

## A Formulae for the condensor with a gap in the upper electrode

### A.1 The parameters $p$ and $\alpha$ as functions of $g/D$

The parameter  $p$  is found by numeric solution of eq.(18). The starting value is not critical.  $\alpha$  is found from  $p$  through eq.(19). Both parameters in their dependence on  $g/D$  are shown in Fig.A.7. Good approximations for these dependences are given by:

$$0.05 \leq g/D \leq 5 :$$

$$p = 1.0702 + 0.0128668 g/D + 1.13868 (g/D)^{1.5} - 0.113642 (g/D)^2;$$

$$\alpha = 0.0929788 g/D + 0.563494 (g/D)^2 - 0.0440619 (g/D)^3.$$

$$5 \leq g/D \leq 20 :$$

$$p = 2.58775 - 4.44539 \sqrt{g/D} + 3.69056 g/D - 0.00420454 (g/D)^2;$$

$$\alpha = -4.70107 + 2.67758 g/D + 0.0102293 (g/D)^2.$$

### A.2 Derivation of the approximate inverse function $f_{3a}^{-1}$

The problem to be treated here concerns models with large gaps between the electrodes; say  $g/D > 3$ , or so. Then far to the left ( $\Re(z) < -g/2$ ) within the condensor ( $0 \leq \Im(z) \leq D$ ) the numeric solution of eq.(19) for a given value of  $z$  runs into trouble; FindRoot[] indicates irrecoverable accuracy loss.

Therefore it was necessary to find an approximate analytic expression valid in this part of the complex  $z$ -plane.

Eq.(19) is rewritten with  $\bar{z} := \pi z/D$  as:

$$\bar{z} + \frac{\alpha}{2} := \hat{z} = \ln t' + \alpha \left(1 - \frac{1}{1+t'}\right) \quad (\text{A.1})$$

$$= \ln t' + \alpha t' - \alpha t'^2 + \dots \quad (\text{A.2})$$

The dangerous part of the  $z$ -plane is mapped to the neighbourhood of  $t' = 0$ . So the lhs. of eq.(A.1) is large as is the logarithm on the rhs. The second term of the rhs. is small as compared to the other terms and is treated as a correction. The smallness of  $t'$  permits one to expand the fraction as shown in eq.(A.2). In the zeroth approximation one gets:

$$t'_{(0)} = e^{\hat{z}} := \beta = e^{\pi z/2D + \alpha/2}.$$

A small correction  $\tau_1$  is added at the rhs. to give  $t'_{(1)}$ . This is inserted into eq.(A.2) after nonlinear powers in  $t'$  have been omitted. After expansion w.r.t.  $\tau_1$  up to the first order one gets:

$$t'_{(1)} = \beta \left(1 - \frac{\beta}{1+\beta}\right).$$

A still smaller correction  $\tau_2$  is added at the rhs. to give  $t'_{(2)}$ . This is inserted into eq.(A.2) with the term  $-\alpha t'^2$  included. The resulting expression is expanded in  $\tau_2$  ( $\tau_1$ ) up to the first (second) order. This gives:

$$t'_{(2)} = \beta \left(1 - \frac{\beta}{1+\beta} + \frac{\beta^2 \alpha(2+\alpha)}{2(1+4\beta\alpha - 2\beta^2\alpha + 5\beta^2\alpha^2 - 2\beta^3\alpha^2 + \beta^3\alpha^3)}\right).$$

Putting all the terms on a common denominator gives eq.(20). The representation above gives insight into the convergence behavior of the iterative procedure. More details can be found in the notebook *SplitCondLW.nb*, subsect.3.5.

## References

- [1] W. Blum, L. Rolandi, Particle Detection with Drift Chambers, Springer, Berlin, 1994.
- [2] W. Riegler, Nucl. Inst. Meth. A 491 (2002) 258; A 535 (2004) 287.

- [3] H.A. Haus, J.R. Melcher, *Electromagnetic Fields and Energy*, Prentice-Hall Inc. Englewood Cliffs, N.J.,1989
- [4] Th. Heubrandtner, *Dissertation*, Technisch-Naturwissenschaftliche Fakultät, Technische Universität Graz, 1999.
- [5] Th. Heubrandtner, B. Schnizer, *Nucl. Inst. Meth.* A478 (2002) 444.
- [6] Th. Heubrandtner, B. Schnizer, H. Schöpf, *Nucl. Inst. Meth. A* 419 (1998) 721.
- [7] B. Schnizer, Th. Heubrandtner, G. Schweitzer, *Nucl. Inst. Meth.* A535 (2004) 454
- [8] J. Van Bladel, *Electromagnetic Fields*, McGraw-Hill Book Comp., New York, 1964.
- [9] G. Schweizer, *Diploma thesis*, Technisch-Naturwissenschaftliche Fakultät, Technische Universität Graz,1995.
- [10] G. Wendt, in: *Encyclopedia of Physics* (S. Flügge, Ed.), vol.XVI, Springer 1958.

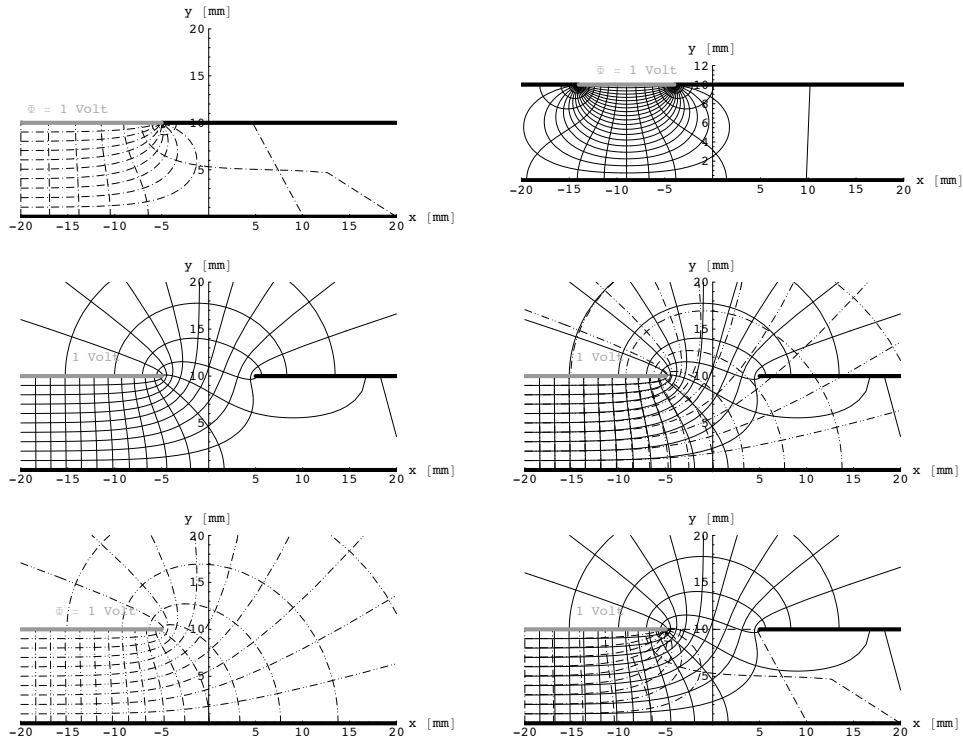


Fig. A.1. Comparison of potential and field distribution in the three models. Condenser width  $D = 10\text{mm}$ , gap widths  $g = 10\text{mm}$ , strip width  $w = 30\text{mm} \gg g$ . The edge under comparison is at  $x = -5\text{mm}$ , so  $b = c = -5\text{mm}$ . Column at left gives the distribution in a single model; from top to bottom: Voltage Strip, Split Condenser, condenser with semiinfinite upper electrode. The upper two pictures show some small inaccuracies for medium or large positive  $x$ : The field lines are not exactly perpendicular to the electrodes; another field line displays a kink. Also the equipotentials may show such defects. These are not very serious since potential and field is rather small at these places. At least a part of them can be remedied by increasing the number of plot points. Right hand column: bottom: Voltage Strip and Split Condenser; middle: seminfinite and Split Condenser. Top: Voltage Strip with a width  $w = 10\text{mm}$  with right edge at  $x = -4\text{mm}$ ; other parameters as before.

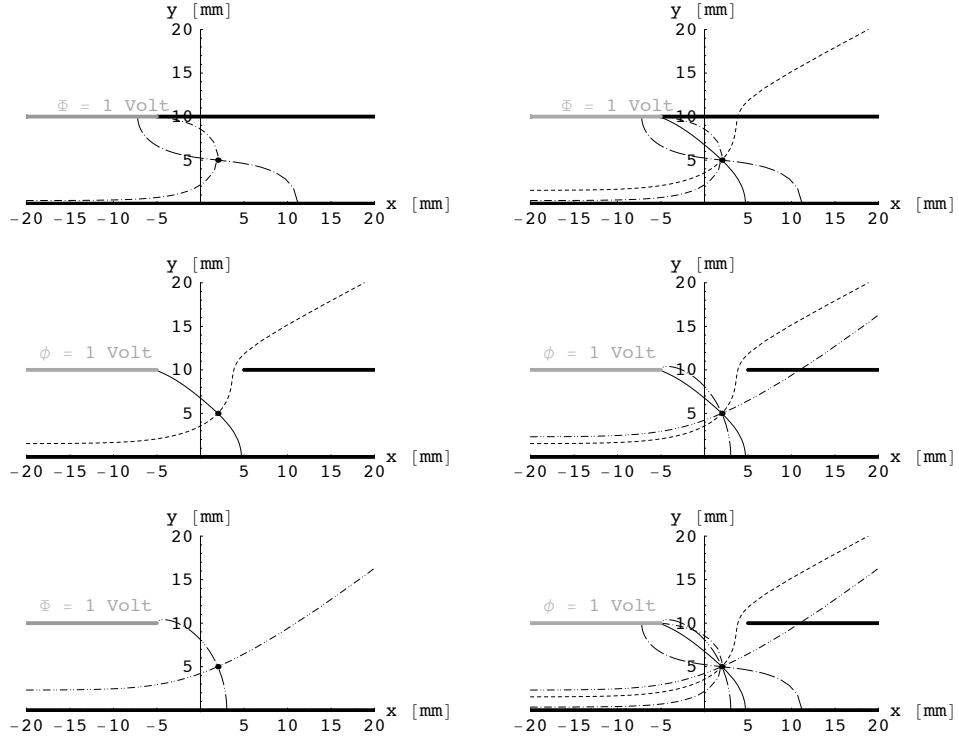


Fig. A.2. Field and equipotential line through a selected point ( $x = 2\text{mm}$ ,  $y = 5\text{mm}$ ) in the three models. Dimensions are the same as in Fig.1. Potential and field values of each model are given below. Column at left gives result for a single model; from top to bottom:

Voltage Strip  $\Phi = 0.035\text{V}$   $(E_x, E_y) = (11.0, -1.2)\text{V/m}$

Split Capacitor  $\Phi = 0.153\text{V}$   $(E_x, E_y) = (28.3, -27.1)\text{V/m}$

semiinfinite upper electrode  $\Phi = 0.231\text{V}$   $(E_x, E_y) = (18.6, -43.1)\text{V/m}$ .

Right column: top: Voltage Strip and Split Capacitor; middle: semiinfinite and Split Capacitor. bottom: all three models together.

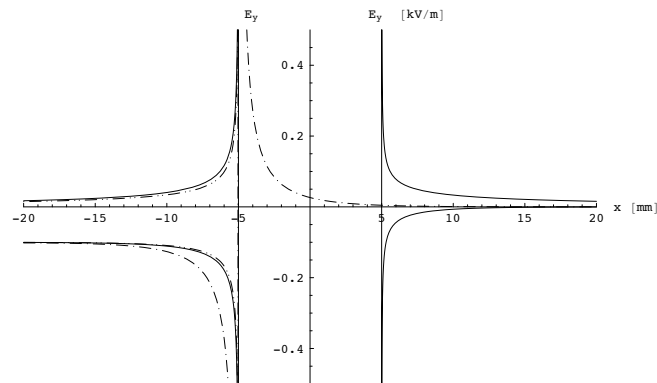


Fig. A.3. Normal electrical field,  $E_y$ , along upper electrode for all three models.  $D = g = 10\text{mm}$ ;  $b = c = -5\text{mm}$ . — Split Condenser, - · - · - condenser with Voltage Strip, - · · - · · -, Semiinfinite condenser .

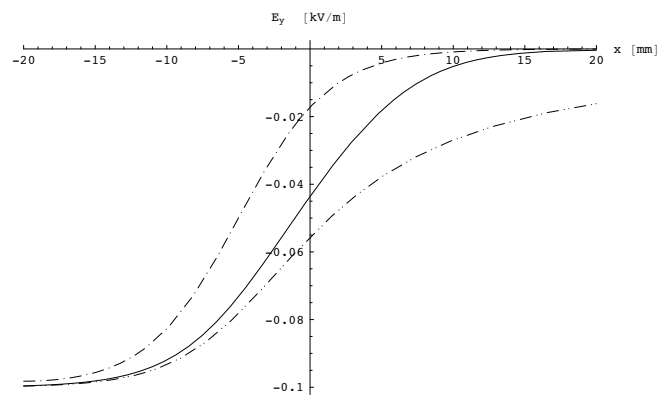


Fig. A.4. Normal electrical field,  $E_y$ , along lower electrode for all three models. Dimensions and dashing the same as in preceding figure.



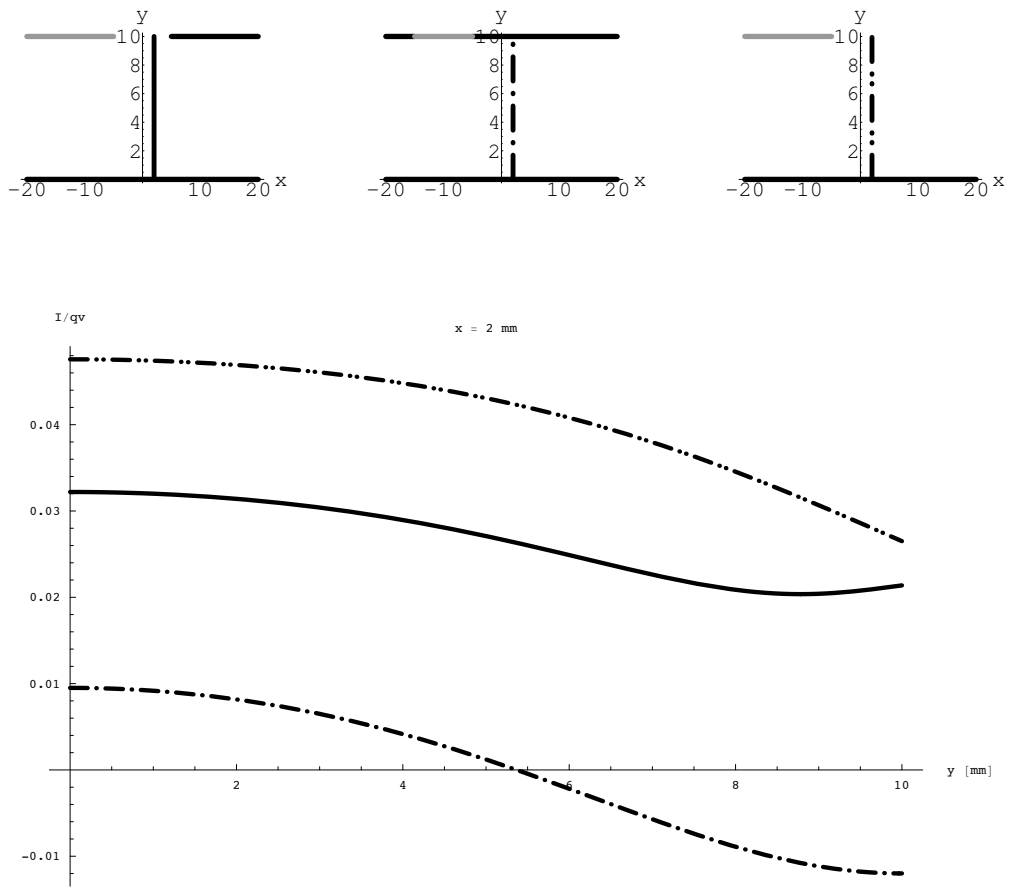


Fig. A.5. Current  $I$  induced in gray electrode of all three models by charge  $q$  moving with velocity  $v$  on trajectory indicated in upper line of figures.  $D = g = 10\text{mm}$ ;  $b = c = -5\text{mm}$ . — Split Condensator, -·-·-·- condensator with Voltage Strip, ······, Semiinfinite condensator .

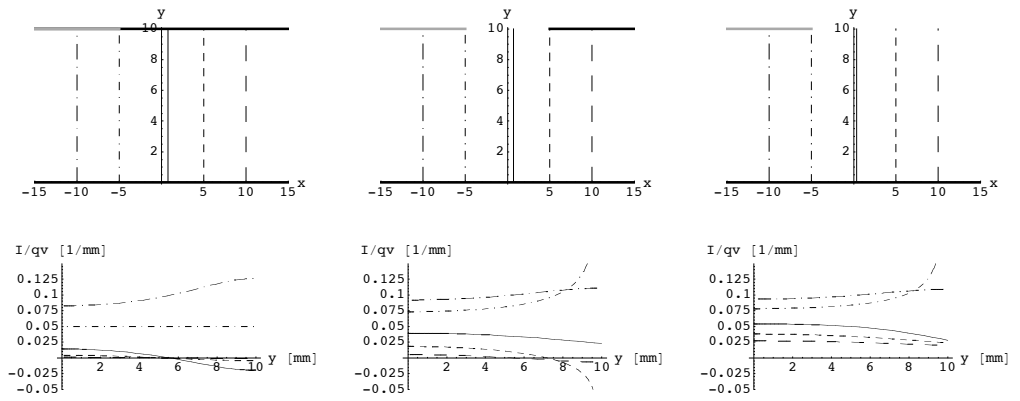


Fig. A.6. Current  $I$  induced in gray electrode of all three models by charge  $q$  moving with velocity  $v$  on trajectories indicated in upper line of figures.  $D = g = 10\text{mm}$ . Corresponding curves have same type of dashed.

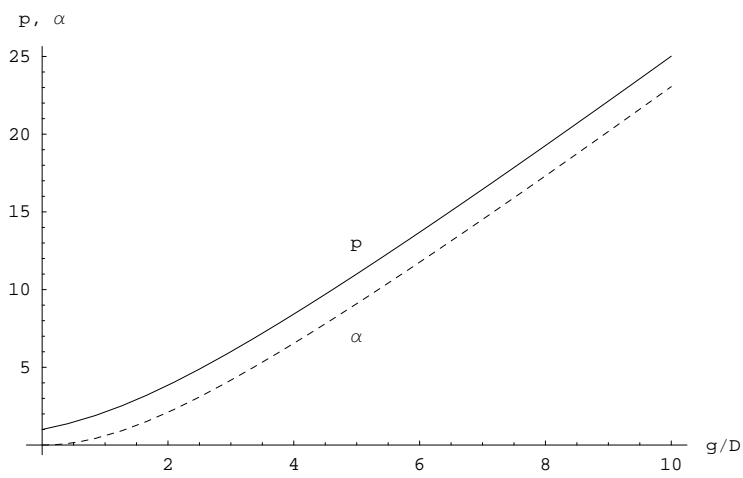


Fig. A.7. The parameters  $p$  and  $\alpha$  versus  $g/D$ .  $D$  is the distance between the two planes containing the electrodes.  $g$  is the width of the gap between the upper two electrodes of the Split Condenser.